Numerical study of vortex-induced vibration by symmetric Lorentz forces

***Hui Zhang, Bao-chun Fan, and Zhi-hua Chen**
Science and Technology on Transient Physics Laboratory, Nanjing University of Science and Technology, China.

*Corresponding author: zhanghui1902@hotmail.com

Key Words: *flow control, vortex-induced vibration, electro-magnetic control, hydrodynamic force*

Abstract

In this paper, the electro-magnetic control of vortex-induced vibration (VIV) of a circular cylinder is investigated numerically based on the stream function-vorticity equations in the exponential-polar coordinates attached on the moving cylinder for Re=150. The effects of the instantaneous wake geometries and the corresponding cylinder motion on the hydrodynamic forces of vortex shedding are discussed in the drag-lift phase diagram. The drag-lift diagram is composed of the upper and lower closed curves, due to the contributions of the vortex shedding, but is magnified, translated and turned under the action of the cylinder motion. The symmetric Lorentz force will symmetrize the flow pass over the cylinder, and decrease the lift oscillation, and in turn, suppresses the VIV.

Keywords: flow control, vortex-induced vibration, electro-magnetic control, hydrodynamic force.

Introduction

Fluid-structure interactions occur in many engineering fields. These interactions give rise to complicated vibrations of the structures and could cause structural damage under certain unfavorable conditions. For a cylinder mounted on flexible supports, the fluctuating forces induced by altering vortex shedding cause the cylinder vibrate. Then, the vibrating cylinder alters the flow field, and in turn changes the flow-induced force. The vibration of the cylinder could increase still further until a limiting behavior has been reached. This vortex-induced vibration (VIV) phenomenon is one of the most basic and revealing problems.

Representative studies carried out experimentally on VIV are the experiments of Feng(1968), Griffin (1980), Griffin & Ramberg (1982)，Brika & Laneville (1993), and Hover (1997) et al, in which classic lock-in was observed, while the shedding frequency coincided with the natural structure frequency. The cylinder experiences significant vibration only with lock-in, and the vibration amplitude has a strong relationship with the phase difference between the lift force and the cylinder motion. However, recently experimental results of Gharib et al(1997), Gharib (1999) and Khalak & Williams (1997) exhibited examples of significant flow-induced vibration without lock-in and suggested whether the VIV with or without lock-in is dependent on the values of the cylinder/fluid mass ratio. Recently, Franzini et al(2009), Lam&Zou(2009) and Korkischko&Meneghini(2010) focus on the interaction of multiple cylinders. It was found that the gap or arrangement has significant effect on the response of the VIV system. Moreover, experimental results of flow around a circular cylinder with moving surface boundary layer control (MSBC) are presented which has the advantages of drag reduction and vibration suppression (Korkischko& Meneghini(2012)).

The progress made during the past two decades on VIV have been reviewed (see. e.g. Willamson&Govardhan (2004) and Sarpkaya (2004)). It is clear that the investigation of fluid-structure interactions as a fully coupled problem are far from complete, there still remain some uncertainties, such as added mass, force decomposition and their effects on the characteristics of the fluid-structure system. Therefore more investigations on an in depth analysis are necessary.

In addition, the control of VIV has many practical applications in the engineering point of view, but a little work has been done on it (Gattulli&Ghanem 1999, Owen et al 2001, Korkischko&

Meneghini(2012)). Therefore, the investigations on the control of VIV are also necessary due to the practical and theoretical importance.

The electro-magnetic control is considered as one of the most practical methods to manipulate the flow (Tang&Aubry 1997, Berger et al 2000, Breuer et al 2004, Mutschke et al 2006, Braun et al 2009). Regarding the flow past a fixed circular cylinder, Crawford and Karniadakis (1995) investigated the effects of Lorentz force on the elimination of flow separation numerically. Weier et al (1998) confirmed the suppressing effect of Lorentz force by both experiments and calculations. Kim&Lee(2001) and Posdziech&Grundmann(2001) found that both continuous and pulsed Lorentz forces can suppress the lift oscillation and stabilize the flow. The closed-loop and optimal control methods were developed to improve its control efficiency in our research group(Zhang et al 2010, Zhang et al 2011), and the suppression of VIV by symmetric Lorentz force was also investigated preliminary(Chen et al 2007).

In this paper, the electro-magnetic control of VIV is investigated numerically. The problems discussed are described by the stream function-vorticity equations in coordinates attached on the moving cylinder, coupled with the cylinder motion equation. A VIV of a cylinder started from rest is controlled by symmetric Lorentz forces after reaching a limiting behavior, and then suppressed till the cylinder vibrates steadily with smaller amplitude. The evolutions of VIV undergoing development and suppression are presented.

Governing equations

For the control of vortex-induced vibration, the cylinder surface consists of two half cylinders mounted with alternating streamwise electrodes and magnets. Obviously, produced Lorentz force is directed parallel to the cylinder surface and decays exponentially in the radial direction, which can be described in dimensionless form (Weier et al 1998, Posdziech et al 2001)

$$\mathbf{F}^* = N\mathbf{F}$$

with

$$F_r = 0$$

$$F_\theta = e^{-\alpha(r-1)} g(\theta) \ \text{with} \ g(\theta) = \begin{cases} 1 & \textit{covered with actuator on upper surface} \\ -1 & \textit{covered with actuator on lower surface} \\ 0 & \textit{elsewhere} \end{cases} \tag{1}$$

where r and θ are polar coordinates, subscripts r and θ represent the components in r and θ directions, respectively. α is a constant, representing the effective depth of Lorentz force in the fluid. The interaction parameter is defined as $N = \dfrac{j_0 B_0 a}{\rho u_\infty^2}$, giving the ratio of the electromagnetic forces to the inertia forces, j_0 and B_0 are the applied electric current density and external magnetic field induction, a is the cylinder radius.

The stream-vorticity equations in the exponential-polar coordinates system (ξ, η), $r = e^{2\pi\xi}$, $\theta = 2\pi\eta$, attached on the moving cylinder, for an incompressible electrically conducting fluid become

$$H\frac{\partial \Omega}{\partial t} + \frac{\partial (U_r \Omega)}{\partial \xi} + \frac{\partial (U_\theta \Omega)}{\partial \eta} = \frac{2}{\mathrm{Re}}\left(\frac{\partial^2 \Omega}{\partial \xi^2} + \frac{\partial^2 \Omega}{\partial \eta^2}\right) + NH^{\frac{1}{2}}\left(\frac{\partial F_\theta}{\partial \xi} + 2\pi F_\theta - \frac{\partial F_r}{\partial \eta}\right) \tag{2}$$

$$\frac{\partial^2 \psi}{\partial \xi^2} + \frac{\partial^2 \psi}{\partial \eta^2} = -H\Omega \tag{3}$$

where the stream function ψ is defined as $\frac{\partial\psi}{\partial\eta}=U_r=H^{\frac{1}{2}}u_r$, $-\frac{\partial\psi}{\partial\xi}=U_\theta=H^{\frac{1}{2}}u_\theta$, while the vorticity Ω is defined as $\Omega=\frac{1}{H}(\frac{\partial U_\theta}{\partial\xi}-\frac{\partial U_r}{\partial\eta})$, with u_r and u_θ the velocity components in r and θ directions, respectively. Furthermore, $H=4\pi^2e^{4\pi\xi}$, $\mathrm{Re}=\frac{2u_\infty a}{\nu}$, u_∞ is the free-stream velocity, ν is the kinematic viscosity, a is the cylinder radius, the non-dimensional time is $t=\frac{t^*u_\infty}{a}$.

The flow is considered to be potential initially and the boundary conditions derived are dependent on the vibrating cylinder. If the cylinder is constrained to move only in cross flow direction, then

$$\text{at } t=0,\quad \psi=0,\quad \Omega=-\frac{1}{H}\frac{\partial^2\psi}{\partial\xi^2}\qquad \text{on } \xi=0$$

$$\psi=-2sh(2\pi\xi)\sin(2\pi\eta),\quad \Omega=0\quad \text{on } \xi>0$$

$$\text{at } t>0,\quad \psi=0,\quad \Omega=-\frac{1}{H}\frac{\partial^2\psi}{\partial\xi^2}\qquad \text{on } \xi=0$$

$$\psi=-\frac{2}{\cos\theta_0}sh(2\pi\xi)\sin(2\pi\eta+\theta_0),\quad \Omega=0\quad \text{on } \xi=\xi_\infty$$

Where $\theta_0=\arctan(-\frac{dl(t)}{dt})$, $\frac{dl(t)}{dt}$ is the velocity of cylinder，the non-dimensional cylinder displacement in the cross-flow direction is $l=l^*/a$.

The shear stress $$\mathcal{C}_\tau^\theta=\mathcal{C}_{\tau F}^\theta+\mathcal{C}_{\tau V}^\theta \tag{4}$$

where $$\mathcal{C}_{\tau F}^\theta=\frac{4}{\mathrm{Re}}\Omega,\quad \mathcal{C}_{\tau V}^\theta=\frac{4}{\mathrm{Re}}\frac{dl}{dt}\cos(2\pi\eta)$$

Therefore, the shear stress can be decomposed into $\mathcal{C}_{\tau F}^\theta$ and $\mathcal{C}_{\tau V}^\theta$, where $\mathcal{C}_{\tau F}^\theta$ is proportional to vorticity at the wall, whereas $\mathcal{C}_{\tau V}^\theta$ induced by the cylinder motion in viscous flow, is independent of vorticity field.

The pressure $$\mathcal{C}_p^\theta=P_\theta-P_\infty=\mathcal{C}_{pF}^\theta+\mathcal{C}_{pW}^\theta+\mathcal{C}_{pV}^\theta \tag{5}$$

where $$\mathcal{C}_{PF}^\theta=\frac{4}{\mathrm{Re}}\int_0^\eta\frac{\partial\Omega}{\partial\xi}\mathrm{d}\eta+\mathcal{C}_p^0,\quad \mathcal{C}_p^0=1+4\pi\int_0^\infty\frac{\partial u_r}{\partial t}e^{2\pi\xi}d\xi+2\int_0^\infty u_\theta\frac{\partial u_r}{\partial\eta}d\xi-4\pi\int_0^\infty u_\theta^2d\xi+\frac{4}{\mathrm{Re}}\int_0^\infty\frac{\partial\Omega}{\partial\eta}d\xi$$

$$\mathcal{C}_{pW}^\theta=4\pi N\int_0^\eta F_\theta\big|_{\xi=0}d\eta,\quad \mathcal{C}_{pV}^\theta=-4\frac{d^2l(t)}{dt^2}\sin(2\pi\eta)$$

Here, pressure $\mathcal{C}_p^\theta$ consists of $\mathcal{C}_{pF}^\theta$ induced by the field Lorentz force, $\mathcal{C}_{pW}^\theta$ induced by the wall Lorentz force and $\mathcal{C}_{pV}^\theta$ induced by the inertial force.

Then the drag C_d can be written as $$C_d=\int_0^{2\pi}\mathcal{C}_d^\theta d\theta=C_{dF}+C_{dW} \tag{6}$$

where $$C_{dF}=\frac{2}{\mathrm{Re}}\int_0^1\left(2\pi\Omega-\frac{\partial\Omega}{\partial\xi}\right)\sin(2\pi\eta)d\eta,\quad C_{dW}=-2\pi N\int_0^1 F_\theta\big|_{\xi=0}\sin(2\pi\eta)d\eta$$

And the lift C_l is written as $$C_l = \int_0^{2\pi} \mathcal{C}_l^{\theta} d\theta = C_{lF} + C_{lW} + C_{lV} \tag{7}$$

where $$C_{lF} = \frac{2}{\mathrm{Re}} \int_0^1 \left(2\pi\Omega - \frac{\partial\Omega}{\partial\xi} \right) \cos(2\pi\eta) d\eta , \quad C_{lW} = -2\pi N \int_0^1 F_\theta \big|_{\xi=0} \cos(2\pi\eta) d\eta$$

$$C_{lV} = -4\pi \frac{d^2 l}{dt^2} - \frac{4\pi}{\mathrm{Re}} \frac{dl}{dt}$$

It is obvious that C_{lW} is independent of flow field. $C_{lW} = 0$, as Lorentz force field symmetric, hence $$C_l = C_{lF} - 4\pi \frac{d^2 l}{dt^2} - \frac{4\pi}{\mathrm{Re}} \frac{dl}{dt} \tag{8}$$

where C_{lF}, so called vortex-induced force, is only dependent on the vorticity and boundary vorticity flux on the cylinder surface. The second term on the right-hand side of the above equation, called inertial force, is only dependent on cylinder acceleration and the third term, called viscous damping force, is dependent on Reynolds number and cylinder velocity. Therefore both second and third terms are independent of the instantaneous flow field.

Non-dimensional mass $m = \frac{m^*}{\pi\rho a^2} = \frac{\rho_{cyl}}{\rho}$, ρ_{cyl} and ρ are the cylinder density and the fluid density respectively; non-dimensional frequency $f = f^* u_\infty / a$ and non-dimensional structure damping $\varsigma = \frac{D}{\pi\rho a u_\infty}$. We may write

$$m \frac{d^2 l}{dt^2} + \varsigma \frac{dl}{dt} + m_{vir} \left(\frac{\omega_n}{\omega} \right)^2 \omega^2 l = F \tag{9}$$

where $F = \frac{C_l}{\pi} = \frac{C_{lF}}{\pi} - \frac{4}{\mathrm{Re}} \frac{dl}{dt} - 4 \frac{d^2 l}{dt^2}$, $\omega = 2\pi f$, f is vortex shedding frequency. At vortex lock-in, the vortex shedding frequency and the natural frequency of the cylinder are synchronized, f_n / f keeps unchanged.

In order to deal with the evolution of the VIV, it is assumed further that the lock-in is kept throughout the developing process of VIV, and then the oscillations of the lift force and the displacement in every motion cycle are represented by a half of peak-to-peak vibration amplitude $\bar{B}$, where $\bar{B}$ is defined by $(B_{upper} + B_{lower})/2$, B_{upper} and B_{lower} are the upper and lower peak values respectively in a motion cycle. Clearly, this assumption does not alter the final steady state of the cylinder vibration. Hence,

$$m_{vir} \left(\frac{\omega_n}{\omega} \right)^2 = m + 4 + \frac{1}{\pi\omega^2} \frac{\bar{C}_{lF_0}}{\bar{B}} \sqrt{1 - \left[\pi\omega \left(\varsigma + \frac{4}{\mathrm{Re}} \right) \right]^2 \left(\frac{\bar{B}}{\bar{C}_{lF_0}} \right)^2} \tag{10}$$

Clearly, m_{vir} changes with time.

The calculations have been performed numerically. The equation of vorticity transport is solved by using the Alternative-Direction Implicit (ADI) algorithm, and the equation of stream function is integrated by means of a Fast Fourier Transform (FFT) algorithm. More details about numerical method and validation of the code can be found in Refs (Tang&Aubry 1997, Zhang et al 2010, Zhang et al 2011). The cylinder motion is calculated by solving equation (10) using the Runge-Kutta method.

Results and discussions

Time evolutions of displacement of VIV cylinder before and after control are shown in Fig.1. Considering a VIV cylinder started from rest, the confinement is released in the cross-flow direction at time t_1, the cylinder begins to vibrate under the action of lift force F , and then tends to reach a limiting behavior. When the symmetric Lorentz force is turned on at time t_2 for a well-developed VIV, the cylinder displacement will decrease with time which is also shown in Fig.1, where the thick solid line and thin dash line represent N=1.3 and N=0.8 respectively. As Lorentz force is strong enough, the separation points disappear completely and the flow becomes symmetric and stable, in turn C_{lF} vanishes and the cylinder will be fixed finally.

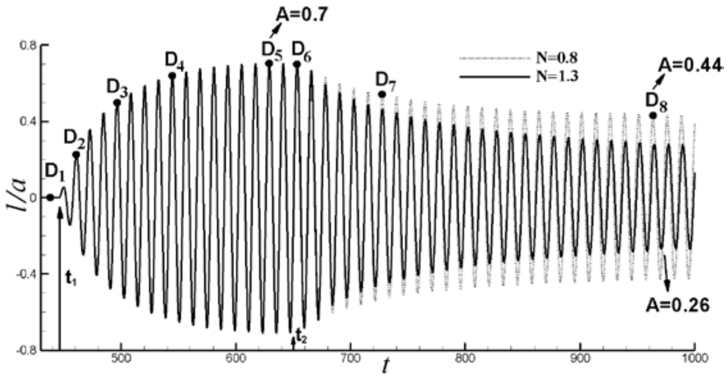

Fig.1 Time evolutions of displacement of VIV cylinder before and after control

Time evolutions of lift C_{lF} and drag C_{dF} for VIV development and suppression are shown in Fig.2. As the cylinder begins to vibrate, the closed curve $A_1B_1C_1D_1A_1$ in Fig.2, representing the stationary cylinder, is turned right with 180^0 due to the effect of the moving cylinder on the shear layer. Subsequently, the mean energy of the cylinder increases as the increase of the cylinder oscillation and the point A separates from the point C, broking the mirrored symmetry of the curve. In addition, the average drag and the amplitude of oscillating lift increase, which causes the diagram magnify and extend continuously from the left to the right as a twisted curve, till VIV is well-developed, and $C_{dF} \sim C_{lF}$ phase diagram is represented by a thick solid line. When the symmetric Lorentz force is applied, the drag C_{dF} induced by the field Lorentz force increases, despite the fact that the total drag C_d does decrease due to the wall Lorentz force effect (Zhang& Fan 2011). Therefore the phase diagram moves to the right dramatically. The flow around the cylinder tends to be symmetric due to the separation suppression, and the lift force C_{lF} decreases, which leads to the decay of the cylinder vibration and the decrease of drag. The phase diagram shrinks and moves to the left as a twisted curve, till the cylinder vibrates steadily with an amplitude smaller than that for well-developed VIV and the point A coincides with the point C again.

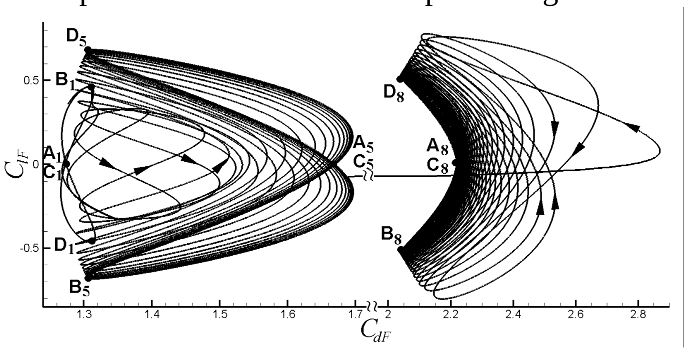

Fig.2 Time evolutions of lift C_{lF} and drag C_{dF} for VIV development and suppression (N=0.8)

The vortex patterns in the wake before and after control by Lorentz force with $N = 0.8$ are shown in Fig.3. All frames correspond to the uppermost cylinder position. The time D_i is expressed in the same instants as used in Fig 1. The cylinder begins to vibrate under the action of lift as the confinement is released at time $t_1 = 446$. Since the energy transfers from the fluid to the cylinder, the cylinder oscillation increases, the corresponding vortex patterns are indicated by $D_1 \sim D_4$. When total energy of cylinder is in the equilibrium state, the cylinder vibrates steadily, the corresponding vortex pattern is indicated by D_5. The control is applied at time $t_2 = 650$, when VIV is well-developed. After control ($D_6 \sim D_8$), the flow in the boundary layer is accelerated under the action of Lorentz force to strengthen the shear layer near the cylinder surface, so that the ability to overcome the adverse pressure gradient is enhanced, which leads to the separation suppression and the wake elongation. Therefore, the separation distance between the upper and lower separation point becomes smaller, and the vortex spaces appear to become wider in stream direction and smaller in the transverse direction.

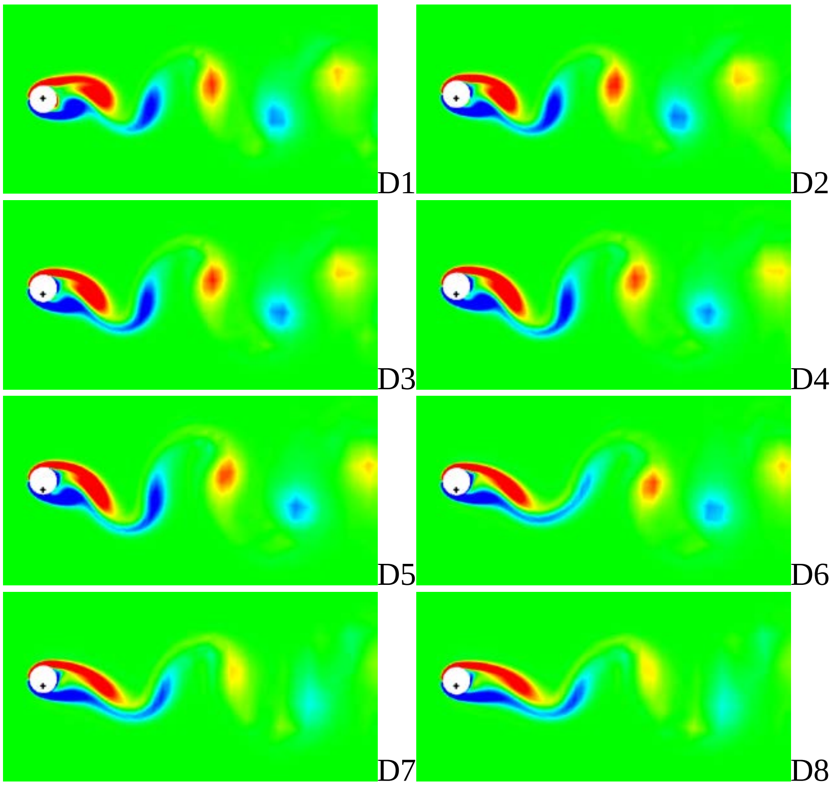

Fig.3 Instantaneous vortex patterns in wake before and after Lorentz force control (N=0.8)

Conclusions

The electro-magnetic control of vortex-induced vibration of a cylinder has been investigated numerically based on the stream function-vorticity equations in exponential-polar coordinates attached on the moving cylinder, and the coupled cylinder motion equation. The initial and boundary conditions together with hydrodynamic forces on the cylinder surface are deduced.

The drag-lift diagram is composed of the upper and lower closed curves, due to the contributions of the vortex shedding. As the cylinder begins to vibrate, the diagram magnify and extend continuously from the left to the right as a twisted curve, till VIV is well-developed. When the symmetric Lorentz force is applied, the phase diagram shrinks and moves to the right as a twisted curve, till the cylinder vibrates steadily with an amplitude smaller than that for well-developed VIV.

The symmetric Lorentz forces can be applied to suppress the VIV. The Lorentz force, being independence of the flow field, is classified into the field Lorentz force and the wall Lorentz force. The wall Lorentz force decreases the drag only and has no effect on the lift, whereas the symmetric field Lorentz force will symmetrize the flow pass over the cylinder, and decrease the lift oscillation, and in turn, suppresses the VIV.

References

Berger, T., Kim, J., Lee, C., Lim, J., (2000), Turbulence boundary layer control utilizing the Lorentz force. Physics of Fluids **12,** pp.631-649.

Braun, E. M., Lu, F. K., Wilson, D. R., (2009). Experimental research in aerodynamic control with electric and electromagnetic fields. Progress in Aerospace Sciences **45,** pp.30-49.

Breuer, K. Park S. J., Henoch, C., (2004). Actuation and control of a turbulent channel flow using Lorentz forces. Physics of Fluids. **16,** pp.897-907.

Brika, D., Laneville, A., (1993). Vortex-induced vibration of a long flexible circular cylinder. Journal of Fluid Mechanics **250**, pp.481-508.

Chen, Z. H., Fan, B. C., Zhou B. M., Li, H Z., (2007). Open loop control of vortex-induced vibration of a circular cylinder. Chinese Physics **16**, pp.1077-1083.

Crawford, C. H., Karniadakis, G. E. (1995). Control of external flows via electro-magnetic fields. AIAA-952185.

Franzini, G.R., Fujiarra A.L.C., Meneghini, J.R., Korkischko, I., Franciss, R., (2009). Experimental investigation of Vortex-Induced Vibration on rigid, smooth and inclined cylinders. Journal of Fluids and Structures **25**, pp.742-750.

Gattulli, V., Ghanem, R., (1999). Adaptive control of flow-induced vibrations including vortex effects. International Journal of non-Linear Mechanics **34**, pp.853-868.

Gharib M. R., Shiels, D. Gharib, M. Leonard, A., Roshko, A., (1997). Exploration of flow-induced vibration at low mass and damping. In Proceedings of Fourth International Symposium on Fluid-Structure Interaction, Aeroelasticity, Flow-Indeced Vibration, and Noise, Vol.1, pp. 75-81. New York: ASME.

Griffin, O. M., (1980). Vortex-excited cross-flow vibrations of a single cylindrical tube. ASME Journal of Pressure Vessel Technology **102**, pp.158-166.

Griffin, O. M., Ramberg S. E., (1982). Some recent studies of vortex shedding with application to marine tubulars and risers. ASME Journal of Energy Research and Technology **104**, pp.2-13.

Gharib, M.R., (1999). Vortex-induced vibration, absence of lock-in and fluid force deduction. Ph.D dissertation, California Institute of Technology, Pasadena, CA, USA.

Hover, F. S., Miller, S. N., Triantafyllou M. S., (1997). Vortex-induced vibration of marine cables: experiments using force feedback. Journal of Fluids and Structures **11**, pp.307-326.

Khalak, A., Williamson, C. H. K., (1997). Fluid forces and dynamics of a hydroelastic structure with very low mass and damping. Journal of Fluids and Structures **11**, pp.973-982.

Kim, S., Lee, C. M., (2001). Control of flows around a circular cylinder: suppression of oscillatory lift force. Fluid Dynamics Research **29,** pp.47-63.

Korkischko, I., and Meneghini, J.R., (2010). Experimental Investigation of flow-induced vibrations at low mass-damping, Journal of Fluids and Structures **11**, pp.973-982.

Korkischko, I., Meneghini, J.R., (2012). Suppression of vortex-induced vibration using moving surface boundary-layer control, Journal of Fluids and Structures **34**, pp.259-270.

Lam, K., Zou, L., (2010). Three-dimensional numerical simulation of cross-flow around four cylinders in an in-line square configuration. Journal of Fluids and Structures **26**, pp.482-502.

Mutschke, G., Gerbeth, G., Albrecht, T., Grundmann, R., (2006). Separation control at hydrofoils using Lorentz forces. European Journal of Mechanics B/Fluids **25,** pp.137-152.

Owen, J. C., Bearman, P. W., Szewczyk, A. A., (2001). Passive control of VIV with drag reduction. Journal of Fluids and Structures **15**, pp.597-605.

Posdziech, O., Grundmann, R., (2001). Electromagnetic control of seawater flow around circular cylinders. European Journal of Mechanics B/Fluids **20**, pp.255-274.

Sarpkaya, T., (2004). A critical review of the intrinsic nature of vortex-induced vibrations. Journal of Fluid and Structures **19**, pp.389-447.

Tang, S., Aubry, N., (1997). On the symmetry breaking instability leading to vortex shedding. Physics of Fluids **9,** pp.2550-2561.

Williamson, C.H.K., Govardhan,.R., (2004). Vortex-induced vibrations, Annual Reviews Fluid Mechanics **36**, pp.413-455.

Zhang, H. Fan, B. C., Chen, Z. H., (2010). Optimal control of cylinder wake by electromagnetic force based on the adjoint flow field. European Journal of Mechanics B/Fluids **29,** pp.53-60.
Zhang, H., Fan, B. C., Chen, Z. H., (2010). Computations of optimal cylinder flow control in weakly conductive fluids. Computers & fluids **39,** pp.1261-1266.
Zhang, H., Fan, B. C., Chen, Z. H., Li, Y. L., (2011). Effect of the Lorentz force on cylinder drag reduction and its optimal location. Fluid Dynamics Research **43**, 015506.